

The Importance of Strongly Bound Pt–CeO₂ Species for the Water-gas Shift Reaction: Catalyst Activity and Stability Evaluation

Danny Pierre  Weiling Deng 
Maria Flytzani-Stephanopoulos

Published online: 27 November 2007
© Springer Science+Business Media, LLC 2007

Abstract We demonstrate ways to prepare active and automotive engine exhausts. Properly stabilized with do- stable Pt–CeO₂ catalysts for the water-gas shift reaction pants, such as rare earth or zirconium oxides, ceria has a (WGSR). Various synthesis protocols are shown to work large oxygen storage capacity and is a suitable carrier of the best being the coprecipitation/gelation method, which platinum and nickel catalysts for the high-temperature suppresses the crystal growth of ceria during calcination by partial oxidation and steam reforming reactions of natural the incorporation of some platinum in the bulk oxide. gas and liquid fuels to produce synthesis gas without car- Metallic platinum nanoparticles are not necessary for arbon deposition [2]. While the high metal dispersion that active WGSR catalyst. Reaction light-off occurs at can be achieved on ceria is not unique to this oxide support, ~ 120 °C, where Pt²⁺ species bound to ceria are still pres- what appears to be unique is the ability of ceria to stabilize ent. No activation period, and no hysteresis phenomoxidized metal species on its surface and subsurface layers were found. During reaction at reducing conditions, some Pt [3–8]. In this article, we review the catalytic properties and is reduced, but it is reoxidizable. The stability of these low-stability of these species for the water-gas shift reaction content (<2 at.%) Pt/CeO₂ catalysts is high even in realistic (WGSR) at low temperatures. This is an important reaction reformat gas streams. To avoid cerium(III) hydroxycar-in fuel processing that enriches the hydrogen content of bonate formation at room temperature-shutdown with watereformate gas streams and removes carbon monoxide, the condensation, a small amount (1%) of gaseous oxygen is latter being a strong poison of the current generation of added to the reaction gas mixture. Cyclic shutdown/startup PEM fuel cell anode catalysts.

Keywords Cerium oxide · Platinum · Water-gas shift
TPR · XPS · Fuel cells · Catalyst deactivation
Carbonate

1 Introduction

Cerium oxide carrying small amounts of Au, Pt, Cu or has focused on evaluating nanoscale Au/ceria catalysts for other metals shows excellent catalytic activity for a variety low-temperature oxidation reactions. After establishing the of redox reactions. As a carrier of Pt-group metals, it is arhigh activity of Au/ceria for the CO and methane oxidation indispensable component of the three-way catalyst in [3, 4], we were rst to show that Au/ceria has very high activity for WGSR [15]. This was subsequently veri ed by several other literature reports, e.g. [6, 17]. A cooperative effect of ceria was invoked to explain why the ceria properties (surface area, crystal size) seemed to matter [15]. More recently, we were able to document the

It is well established in the literature that addition of Pt metals on ceria dramatically enhances the reducibility of the surface oxygen of ceria. This was shown more than 20 years ago by Yao and Yu Yao [9]. Pt-group metals supported on a high surface area ceria are much more active for the CO oxidation [10] and the WGSR [7, 11] than if loaded on annealed microcrystalline ceria or on alumina, as was shown by the Gorte's group. The same is true for CuO/CeO₂ [3, 4, 12–14]. In recent years, our group

D. Pierre · W. Deng · M. Flytzani-Stephanopoulos (✉)
Department of Chemical and Biological Engineering,
Tufts University, 4 Colby St., Medford, MA 02155, USA
e-mail: maria.ytzani-stephanopoulos@tufts.edu

importance of the interaction between gold and the oxygen the full gas mixture with water condensation. The problem of ceria [7, 8, 18] by showing that only the gold species lies with ceria, which forms Ce (III) hydroxycarbonate embedded or otherwise associated with ceria, [Au–Ce] under these conditions [8]. Doping ceria with zirconia was are the active sites for WGS [7]. The number of these found to improve the stability of undoped ceria [29]. While bound gold species that can be carried by ceria is increased activity can be recovered by reoxidation of the catalyst in as the crystal size of ceria is decreased [9]. Similarly, air at high temperatures (>450 °C) [8, 29], this scheme is oxidized clusters of Pt bound to ceria, [Pt–Ce], were not practical in a continuous operation of a fuel cell system. found after removing the platinum nanoparticles from the A practical, in situ remedy of the deactivation problem ceria surface by cyanide leaching; and all the platinum had of ceria upon WGS shutdown was proposed earlier this diffused in the subsurface layers of ceria [19]. In earlier year by Deng et al. [31]. This was based on the information work, we had noticed similar effects with the Cu/ceria that Au/CeO₂ is an excellent catalyst for the preferential oxidation catalysts; namely, that only a small amount of CO oxidation reaction (PROX) [32] and is not deactivated copper (<2 at.%) strongly bound to ceria (non-leachable) in cyclic shutdown/startup PROX operation when exposed was responsible for the CO oxidation reaction [4]. to practically the same gas mixture as for WGS, except for

A novel synthesis approach aimed at demonstrating the presence of gaseous oxygen. Addition of a small maximizing the interaction between Pt and ceria was amount of oxygen in the WGS reaction gas mixture was reported by Tsang's group in 2003 [30]. Encapsulation of then tried and shown to prevent the Ce (III) hydroxycar-platinum particles inside a nanoscale shell of ceria was sonate formation. Full stabilization of the Au/ceria catalyst achieved by a reverse microemulsion technique. This was demonstrated both in continuous operations at tem- resulting material showed excellent activity for the WGS peratures up to 300°C, and in cyclic room temperature reaction, while the undesired methanation reaction was shutdown/reheat to 150 or 300°C [31, 33]. suppressed by not exposing the metallic Pt sites.

Nanoscale ceria has a much higher concentration of design of novel ceria-based catalysts for WGS reactors surface oxygen defects than microcrystalline ceria and coupled to fuel cell systems with a two-prong objective: (i) much higher conductivity. This is true both for the bulk to investigate ways to increase the amount of fully bound material [21] as well as for thin films of ceria [22]. The Pt- or Au- on ceria, which would in turn increase the rate of surface Ce–O bond is weakened by the presence of a metal the WGS; and (ii) to examine the catalyst activity and and this oxygen becomes reactive at low temperatures stability in realistic reaction gas streams and in cyclic Addition of gold, platinum, etc. increases the available operation, including shutdown to ambient conditions. In oxygen on the surface, if preparation conditions are proper the present paper we show this for Pt–CeO₂ catalysts. early controlled. Recently, the Corma group has also reported on the importance of nanoscale ceria and characterized the types of excess active oxygen on the surface of gold/nanocerium materials [23, 24].

Deactivation with time-on-stream and/or shutdown/re-startup operation has been reported for WGS catalysts based on ceria [8, 25–29] or copper oxide [30]. The noble metal/ Lanthanum-doped ceria and undoped ceria materials were ceria materials are superior to commercial low-temperature prepared by the urea gelation/co-precipitation (UGC) shift catalysts based on Cu/ZnO in that they are non-pyromethod. Details about this preparation technique can be phoric, do not require activation, do not catalyze the found elsewhere [7, 13]. Low-content platinum–ceria methanation reaction; and are thus a better candidate for samples were prepared by one-pot synthesis using UGC, application to small-scale fuel cells, undergoing frequent air and by incipient wetness impregnation (IMP), and depurges. However, deactivation of the Pt metal/ceria catalyst–precipitation (DP) on ceria particles prepared by the catalysts with time-on-stream in realistic reformate-gas streams UGC method and calcined at 400°C. All reagents used in has been reported and attributed to various reasons, such as catalyst preparation were analytical grade. The samples metal-induced over-reduction of ceria [26], precious metal reported here are denoted as a%PtCeO₂a%PtCeLaO₂ sintering after high-temperature reaction aging of Pd and Pt where a is the atomic percent of platinum in the sample: CeO₂ catalysts [27] and carbonate formation [28]. Finally, a 100 × (Pt/MW_{Pt})/(Pt/MW_{Pt} + Ce/MW_{Ce} + La/MW_{La}), different type of deactivation was found in cyclic operation, CeLaO₂ is ceria doped with 10 at.% La. mimicking the frequent shutdowns to room temperature For IMP samples, the ceria support was impregnated followed by re-start of a realistic fuel cell system. Severe with a solution of chloroplatinic acid at room temperature deactivation due to carbonate formation has been reported (RT). A measured amount of solution carrying the required both for Pt/CeO₂ [29] and Au-ceria [8, 19] after shutdown in metal ion concentration was added dropwise to fill the pore

volume of the solid support. This was followed by drying

the material in a vacuum oven at 60 °C for 10 h to remove

water and allow good coating of the metal precursor on the pore surface. The dried material was calcined at 400 °C for 10 h.

In the DP method, two different platinum precursors were used: tetra-ammine platinum(II) nitrate, for 0.5 h before starting the TPR at a rate of 5 °C/min from (NH₃)₄Pt(NO₃)₂, and hydrogen hexachloroplatinate(IV) hydrate, H₂PtCl₆. In both cases, the solution containing the desired amount of platinum was added dropwise into an aqueous slurry of a previously UGC-prepared ceria. Prior to this addition, the pH of the slurry was adjusted to 2 (NTP) at 350 °C for 30 min; cooled to RT in the oxygen before adding H₂PtCl₆ using 1 M HNO₃ and to 12 before adding (NH₃)₄Pt(NO₃)₂ using 1 M NaOH, respectively.

After aging for 1 h, the precipitate was filtered and washed with deionized water. The resultant material was then dried and calcined as described above.

Some materials were leached with 2% NaCN–NaOH solution (pH > 12) at ~90 °C in an oil bath for 24 h [7] to remove weakly bound platinum species from the ceria surface. Leached samples were washed with deionized water three times; dried in a vacuum oven for 10 h and heated in air at 400 °C for 2 h.

2.2 Characterization Techniques

The BET surface area was measured by single-point

adsorption/desorption cycles in a Micromeritics Pulse

ChemiSorb 2705 flow apparatus. Bulk composition analy-

sis of the catalysts was conducted in an Inductively

Coupled Plasma Optical Emission Spectrometer (ICP-OES,

Leeman Labs Inc.). XPS and XRD analyses were per-

formed at the MIT Center for Materials Science and

Engineering. For XPS, a Kratos AXIS Ultra Imaging X-ray Table

Photoelectron Spectrometer with a resolution of 0.1 eV

was used to determine the atomic metal ratios of the sur-

face region and the oxidation state of platinum in selected

UGC-catalysts. Samples in powder form were pressed on

double-side adhesive copper tape for analysis. All mea-

surements were carried out at room temperature without

any sample pre-treatment. An Al K_α X-ray source was used

in this work. All binding energies were adjusted to the C 1s

peaks at 285 eV. An adjacent neutralizer was used to

minimize the static charge on the samples. XRD analysis

was performed on a Rigaku 300 instrument with a rotating

anode generator and a monochromatic detector. Cu K

radiation was used with a power setting of 60 kV and

300 mA. Typically, a scan rate of 2°/min with 0.02°

interval was used. Tungsten was used as an internal sta-

ndard. The software TOPAS (Bruker) was used to perform

microstructure analysis.

2.3 Testing Apparatus and Procedures

Temperature-programmed reduction by hydrogen₂- (H

TPR) was conducted in a Micromeritics Pulse ChemiSorb

2705 instrument equipped with a thermal conductivity

detector to detect H₂ consumption. The as prepared mate-

rials (0.5 g sample) in the powder form were purged in He

for 5 min from

RT to 400 °C in a 20% H₂/N₂ gas mixture (50 cm³/min

(NTP)). In cyclic H₂-TPR experiments, a He sweep

immediately followed the first TPR test, the sample was

reoxidized in the 20% O₂/He gas mixture (50 cm³/min

at 350 °C for 30 min; cooled to RT in the oxygen

gas mixture; then purged in He before starting the second

TPR cycle.

WGS tests were conducted at atmospheric pressure

with the catalyst in powder form (150 μm). A quartz tube

(o.d. = 1 or 0.5 cm) with a porous quartz frit supporting

the catalyst was used as a packed-bed flow reactor. Water

was injected into the flowing gas stream by a calibrated

syringe pump and vaporized in the heated gas feed line

before entering the reactor. A condenser filled with ice was

installed at the reactor exit to collect water. The feed and

product gas streams were analyzed by a HP-6890 gas

chromatograph (GC) equipped with a thermal conductivity

detector (TCD). A Carbosphere (Alltech) packed column

(6 ft × 1/8 in.) was used to separate CO, H₂, and CO₂.

No methane was produced under any of the operating

conditions used in this work.

Flow apparatus. Bulk composition analy-

sis of the catalysts was conducted in an Inductively

Coupled Plasma Optical Emission Spectrometer (ICP-OES,

Leeman Labs Inc.). XPS and XRD analyses were per-

formed at the MIT Center for Materials Science and

Engineering. For XPS, a Kratos AXIS Ultra Imaging X-ray Table

Photoelectron Spectrometer with a resolution of 0.1 eV

was used to determine the atomic metal ratios of the sur-

face region and the oxidation state of platinum in selected

UGC-catalysts. Samples in powder form were pressed on

double-side adhesive copper tape for analysis. All mea-

surements were carried out at room temperature without

any sample pre-treatment. An Al K_α X-ray source was used

in this work. All binding energies were adjusted to the C 1s

peaks at 285 eV. An adjacent neutralizer was used to

minimize the static charge on the samples. XRD analysis

was performed on a Rigaku 300 instrument with a rotating

anode generator and a monochromatic detector. Cu K

radiation was used with a power setting of 60 kV and

300 mA. Typically, a scan rate of 2°/min with 0.02°

interval was used. Tungsten was used as an internal sta-

ndard. The software TOPAS (Bruker) was used to perform

microstructure analysis.

presence of Ce³⁺, which is a larger ion than Ce⁴⁺, its

Table 1 Physical properties of platinum–ceria materials

Sample	BET S.A.(m ² /g)	Bulk composition(at. %)			Surface composition (at. %)			Crystallite size ^d (nm)		Lattice constant(A)		
		Pt	Ce	La	Pt	Ce	La	CeO ₂		CeO ₂		
								<111>	<220>	<111>	<220>	
2.2%PtCeLaQ(IMP)	151.1	2.20	89.32	8.48	NM	NM	NM	ND	5.2	5.0	5.422	5.422
0.7%PtCeLaQ(IMP,NaCN)	162.9	0.74	90.71	8.55	NM	NM	NM	ND	5.3	5.0	5.432	5.432
1.2%PtCeQ(IMP)	156.0	1.22	98.78	0	0.59	99.41	0	ND	6.3	7.6	5.417	5.415
0.8%PtCeQ(DP,pH2)	144.0	0.82	99.20	0	0.51	99.49	0	ND	6.4	7.8	5.413	5.421
0.8%PtCeQ(DP,pH2) ^f	119.0	0.82	99.20	0	0.62	99.38	0	ND	6.6	7.9	5.435	5.418
0.3%PtCeQ(DP,pH12)	140.0	0.30	99.70	0	0.12	99.88	0	ND	6.6	7.5	5.418	5.416
5.3%PtCeQ(UGC)	140.7	5.32	94.68	0	3.5	96.5	0	ND	3.7	3.2	5.413	5.436
5.3%PtCeQ(UGC) ^f	NM	5.32	94.68	0	3.5	96.5	0	ND	3.8	3.5	5.431	5.473
1.1%PtCeQ(UGC)	167.9	1.07	98.93	0	0.95	99.05	0	ND	5.1	4.6	5.442	5.401
CeLaQ(UGC)	156.9	0	92.62	7.38	0	ND	ND	–	5.1	4.8	5.438	5.442
CeO ₂ (UGC)	140.5	0	100	0	0	100	0	–	7.1	6.6	5.415	5.416

^a All samples calcined at 400°C in air for 10 h, except the leached samples for 2 h

CeLaQ: 10 at.%La-doped ceria, calcined at 400, 10 h; ND: non-detectable; NM: not measured

^b Bulk composition was determined by Inductively Coupled Plasma (ICP) emission spectrometry

^c Surface composition was determined by XPS

^d The crystallite size was determined from XRD data with the Scherrer equation

^e The lattice constant was determined by the expression $\sqrt{h^2 + k^2 + l^2}(\lambda/2 \sin \theta)$

^f Sample was used for 17 h at 300 in the reaction gas mixture of 11%CO–26%O₂–26%H₂–7%CO₂–He

fraction increasing as the size of nanoscale ceria is both UGC samples have a mix of Pt²⁺ and Pt⁴⁺ (binding energy at 74.0 and 77.4 eV). All of them have negligible Pt⁰ (binding energy at 70.9 and 74.3 eV). The higher content DP, IMP, and UGC methods contain oxidized Pt species as 5.3%PtCeQ(UGC) sample still shows all of its platinum in identified by XPS in Fig. 1. 0.8%PtCeQ (DP), 2⁺ and 4⁺ oxidation states. This is the sample with the smallest average particle size of ceria (Table) The surface Pt²⁺ species (binding energy at 72.6 and 76.0 eV) while the surface platinum content of the samples was also determined by XPS and can be seen in Table. The fraction of Pt on the surface is less than the bulk value. A lot of platinum is sub-surface in ceria, even in the sample prepared with 5.3% Pt by the UGC technique. No platinum phases were detected by XRD in any of the PtCeQ samples shown in Table, including the high content 5.3%PtCeQ indicating the platinum is present in highly dispersed small clusters in cerium oxide. Taken together the XPS data of Fig. 1 and the sample analysis of Table, provide evidence that the as prepared materials comprise oxidized platinum clusters strongly bound to nanoscale ceria.

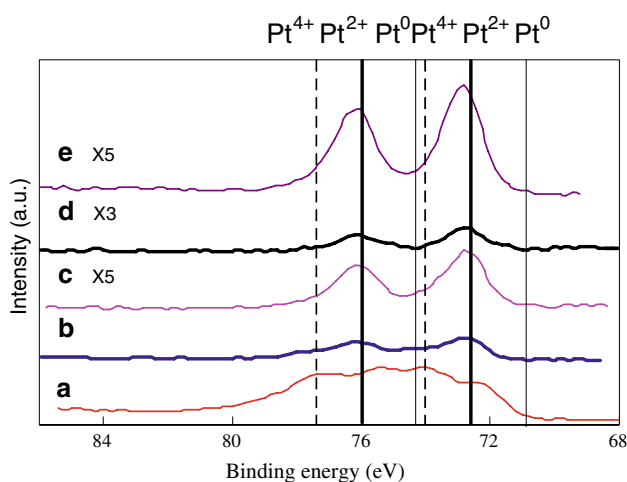


Fig. 1 XPS of Pt_{4f}–Pt–CeQ samples, as prepared, after air calcination at 400°C. (a) 5.3%PtCeQ(UGC); (b) 1.1%PtCeQ(UGC); (c) 0.8%PtCeQ (DP, pH₂); (d) 0.3%PtCeQ (DP, pH₁₂); (e) 1.2%PtCeQ (IMP). X5 and X3 is signal magnification

3.2 WGS Reaction Activity and Stability

Figure 2 shows steady-state CO conversions in the WGS reaction over the platinum–ceria catalysts prepared by different methods in a product-free feed gas mixture containing 2%CO and 10.7%O₂ in helium. For each run,

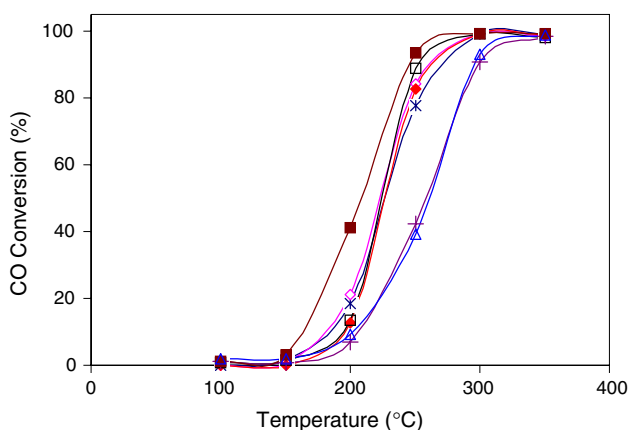


Fig. 2 WGS reaction light-off over platinum–ceria catalysts; steady-state conversion measurements. Gas mixture: 2%CO–10% H_2 –11% CO_2 –26% H_2O –bal.He; contact time: 0.09 g s/cc. Open Triangles—2.2%PtCeLaQ (IMP); Open squares—0.7%PtCeLaO (IMP, NaCN); Asterisks—0.8%PtCeQ (DP, pH2); Open diamonds—1.2%PtCeQ (IMP); Crosshairs—0.3%PtCeQ (DP, pH12); Closed Squares—5.3%PtCeQ (UGC); Closed diamonds—1.1%PtCeQ (UGC)

0.1 g sample was tested in ascending temperature mode (50 °C-increments) followed by descending temperature to 250 °C. Of course, this is only an approximate value, as the surface amount and the dispersion of platinum may vary with time-on-stream for some or all of these samples. But it is interesting that all samples have similar TOFs and also similar apparent activation energies, $E_a = 81.0 \pm 6.8$ kJ/mol. If we compare the ceria properties of the catalysts

at the conditions of Fig. 2. At 300 °C, the CO conversion was at least 90% over all catalysts.

We further evaluated the catalysts in a realistic reformate gas composition. It is of interest both from a practical as well as a fundamental point of view to check the activity and stability of these PtCeQ samples in a gas with a large content of hydrogen and also in the presence of CO_2 . Table 2 shows the steady-state reaction rates measured at 250 °C over these catalysts at CO conversions less than 20% to avoid mass transfer effects. The IMP samples are similarly active. The UGC samples have good rates, the 5.3%PtCeQ sample showing the highest rate, which we attribute to the higher amount of Pt present in active form in this sample. If we normalize the rates by the surface amount of Pt measured by XPS on the as prepared samples, as a first-order approximation, we can calculate the turnover frequencies (TOF) of the reaction. Since by XRD no diffraction pattern was found for Pt in any of the samples and the XPS analysis found all the platinum in oxidized form, the TOF calculation assumed that the surface Pt

determined by XPS was fully dispersed (see foot notes in Table 2). As shown in the last column of Table 2, a value of $TOF = 0.15 \pm 0.06$ s⁻¹ is found for all samples at 250 °C. Of course, this is only an approximate value, as the surface amount and the dispersion of platinum may vary with time-on-stream for some or all of these samples. But it is interesting that all samples have similar TOFs and also similar apparent activation energies, $E_a = 81.0 \pm 6.8$ kJ/mol. If we compare the ceria properties of the catalysts

Table 2 WGS reaction activity measured in a reformate gas mixture

	Apparent activation energy (kJ/mol)	Reaction rate ($\mu\text{mol CO}_2/\text{g}_{\text{cat}}/\text{s}$)	TOF ^e (s ⁻¹)
2.2%Pt CeLaQ (IMP)	80.7	7.2	N/A
0.7%Pt CeLaQ (IMP,NaCN)	84.9	6.5	N/A
1.2%PtCeQ (IMP)	83.2	5.7	0.17
0.8%PtCeQ (DP,pH2)	85.8	4.0	0.13
0.3%PtCeQ (DP,pH12)	72.7	1.5	0.21
5.3%PtCeQ (UGC)	85.4	20.7	0.10
1.1%PtCeQ (UGC)	84.6	6.2	0.11
3.7%PtCeLaQ (IMP) ^b	74.2	10.0	0.11
2.7%PtCeLaQ (IMP,NaCN) ^b	75.2	16.1	0.16
1.5%PtCeLaQ (IMP,NaCN) ^b	75.0	6.3	0.21
CeLaQ (UGC)	82.7	0.02 ^d	–

^a 11%CO–8%CO₂–26% H_2 –26% H_2O –bal.He

^b Data adapted from Ref. [7]

^c 250 °C, 1 atm

^d Rate extrapolated from high temperature rate measurements

^e Turnover frequency; based on the initial amount of surface Pt species found by XPS, see Table 1. $TOF(s^{-1}) = r \left(\frac{\text{mol}}{\text{g}_{\text{cat}} \cdot \text{sec}} \right) * \left(\frac{\text{g}_{\text{cat}}}{\text{mass of Pt on cat surface}} \right) * \left(\frac{M_w \text{ of Pt}}{\text{Fraction of surface atoms}} \right)$

listed in Table 1, the particle size of CeO_2 a key variable. The samples prepared by the UGC method have the smallest cerium oxide particle size and can retain more oxidized platinum species on their surface and sub-surface layers which correlates well with their higher reaction activity. Similar results were reported for gold/ceria catalysts [7, 8, 15]. A much higher WGS activity of Pt-metals deposited on nanoscale ceria films was first reported by the Gorte group [1].

The activity and stability of some of the above catalysts was further evaluated in the same WGS gas mixture (11% CO –26% H_2O –26% H_2 –7% CO_2 –He) at 300°C for 17 h. As can be seen in Fig. 3a, the stability of Pt/CeO₂ is generally very good. Unlike what has been reported in the literature for some other Pt/CeO₂ catalysts [26], no drastic initial deactivation is observed for any of the samples shown in Fig. 3a. However, there are some activity differences among our samples that can be traced to the different preparation and structure. The 0.7%PtCeLaO (IMP, NaCN) and 0.8%PtCeQDP catalysts appear less active and stable than the 1.1%PtCeQ (UGC) and the 1.2%PtCeQ (IMP) sample. The CO conversion falls from ~60% to ~50% over 17 h for the former two catalysts, while it remains constant at 80% for the latter. The best performance is shown by the 5.3%PtCeQ (UGC) sample, which reaches the equilibrium CO conversion of 92%, and shows excellent stability with time-on-stream at 300°C.

XP Pt_{4f} spectra of the fresh and used 0.8%PtCeQDP catalyst are shown in Fig. 3b. Some metallic Pt is now found in the used sample. Peak deconvolution shows that over 50% of the Pt is still in oxidized form. The BET surface area of the used sample is 11% lower than the initial value of 144 m²/g. (Table 1). This may explain the ~20% loss in activity. The lattice constant is higher in the used catalyst indicating that a higher amount of Ce is likely present in the used than the fresh sample causing lattice expansion as discussed above.

Figure 3c presents the XP Pt_{4f} spectra for the as prepared and used 5.3%PtCeQ (UGC) catalyst. The used sample lost most of its Pt⁴⁺ species. Pt⁰ species now dominate, while no metallic platinum has formed. This sample is the most active and stable under the conditions of Figs. 2 and 3. The absence of Pt⁴⁺ has no effect on the catalyst stability. Thus, Pt⁴⁺ species are responsible for the observed catalyst activity. Comparing these data with the 0.8%PtCeQ (DP) catalyst, we can surmise that the deactivation of the latter with time-on-stream (Fig. 3a) is due to accumulation of Pt⁰ (Fig. 3b). Metallic platinum may in turn cause the annealing of ceria oxygen vacancies and the loss of ceria surface area.

From the above evaluation, the catalyst that consistently showed the best activity and stability is the UGC-prepared 5.3%PtCeQ. This has the smallest particle size of ceria

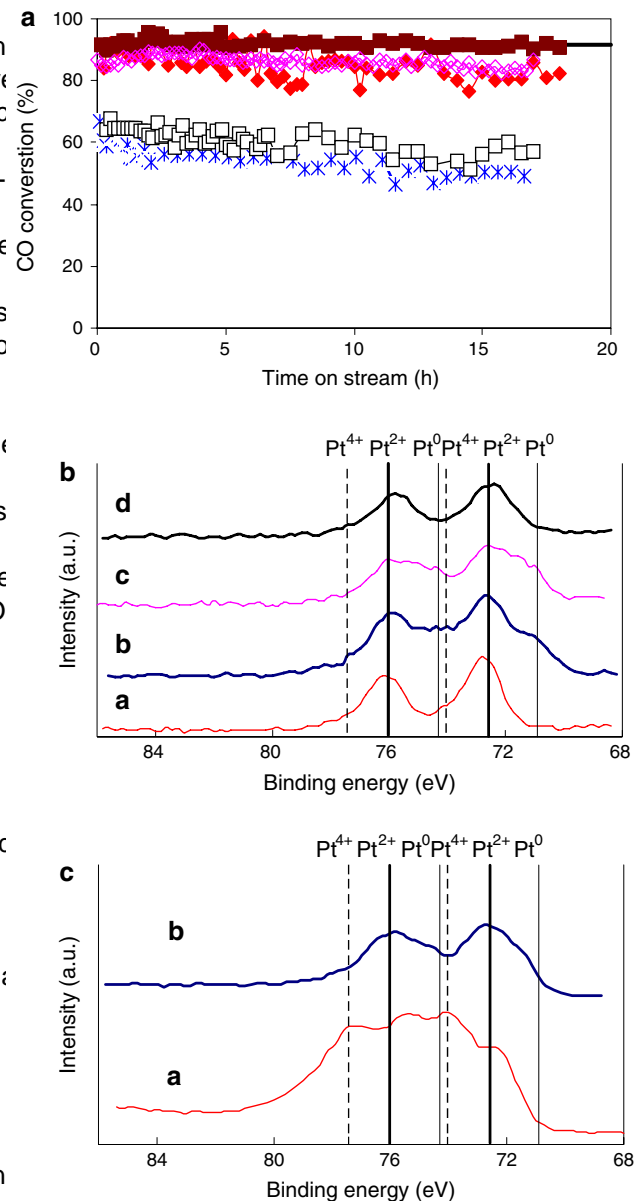


Fig. 3 (a) WGS stability of PtCeQ catalysts at 300°C. Gas mixture: 11% CO –26% H_2O –26% H_2 –7% CO_2 –He; sample load 0.5 g; S.V. = 50,000/h (NTP). Solid line—Equilibrium conversion; Open squares—0.7%PtCeLaO (IMP, NaCN); Open diamonds—1.2%PtCeQ (IMP); Asterisks—0.8%PtCeQDP, pH₂; Closed squares—5.3%PtCeQ (UGC); Closed diamonds—1.1%PtCeQ (UGC). (b) XPS of Pt_{4f}—0.8%PtCeQ (DP, pH₂). (a) as-prepared; (b) used at the conditions of (a), after 17 h at 300°C; (c) after H₂-TPR; (d) reoxidized after H₂-TPR by oxygen at 350°C for 0.5 h. (c) XPS of Pt_{4f}—5.3%PtCeQ (UGC). (a) as-prepared (b) used at the conditions of (a), after 17 h at 300°C

(Table 1) and can stabilize more platinum in the desired strongly bound Pt–O–Ce form. Similar to what we have

previously reported for Au on nanoscale CeO₂ [8, 15], the UGC preparation method increases the concentration of these species and higher reaction rates are possible. The

TOF of the WGS reaction measured at 250s the same for all samples (Table 2).

3.3 Reducibility in H₂

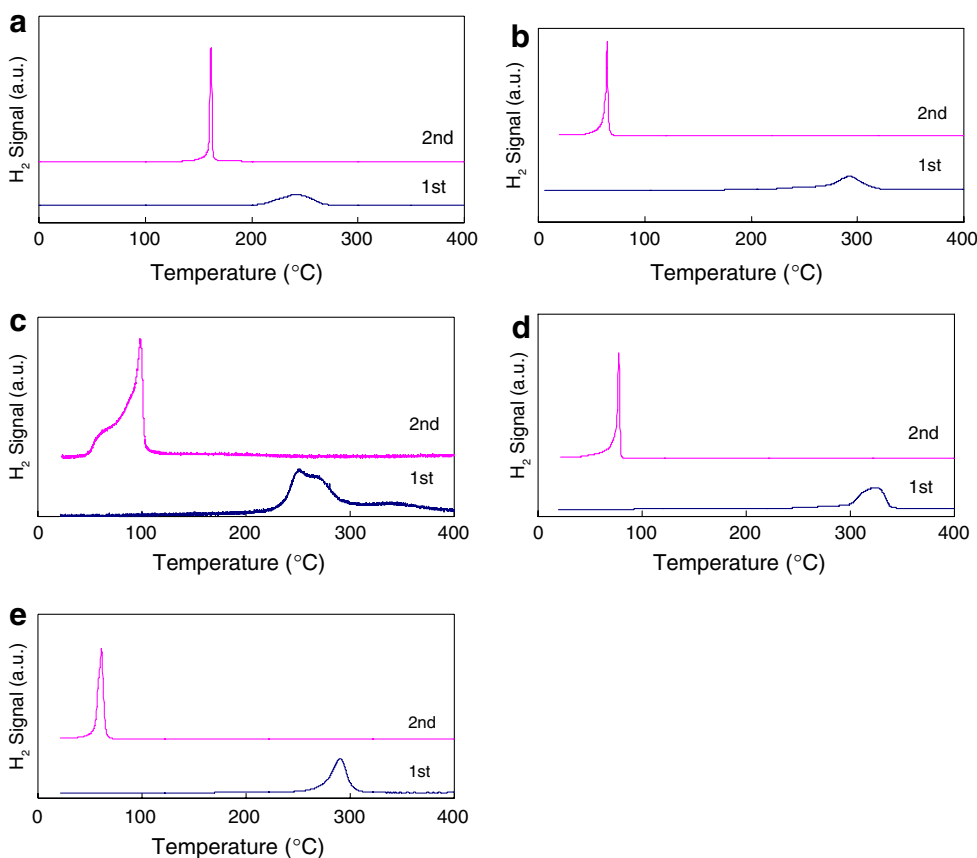
It is of interest to evaluate the reducibility of the Pt–CeO catalysts and investigate the potential correlation of their distinguishable. Reduction peak temperatures are listed in Table 3 for the first and second cycles of H₂-TPR. The subject is rather confusing. The effect of weakening the second TPR cycle is typical for metallic Pt on ceria, as can be seen by the very sharp, low-temperature (100 °C) reduction peaks. A third cycle (not shown) was similar to reports ever since it was first demonstrated by Yao and Yuh to Yao [9]. However, over-reduction of ceria may not always be advantageous. While the presence of metallic platinum on ceria materials [8], the reduced platinum–ceria samples can and gold nanoparticles on ceria causes a dramatic reduction of the surface oxygen of ceria to water vapor.

temperatures below 100 °C, oxidized species of Pt and Au strongly bound to ceria are less reducible [8, 15, 19, 20]. Yet, that does not mean that the latter are less active. On the contrary, these rather than the metallic Au or Pt nanoparticles are the active species for some redox reactions, such as the WGS [7]. For other reactions, such as the CO oxidation reaction by dioxygen, the opposite may hold true [36].

None of the samples prepared here contains metallic platinum as verified also by H₂-TPR, in Figs. 4 and 5, which show absence of the characteristic low-temperature reduction peak. Instead, oxygen reduction begins at temperatures approaching or higher than 200 °C. An exception is seen in Fig. 5a for 5.3%PtCeQ which begins to reduce

The presence of metallic platinum after the first TPR cycle was checked by XPS on the 0.8%PtCeQ (DP) sample. As can be seen in Fig. 6, line c, after the test in H₂-TPR up to 400 °C, the Pt 4f binding energies shifted to lower values, indicative of metallic Pt formation. A third cycle (not shown) was similar to the second. Thus, after the first treatment in H₂ up to 400 °C, metallic Pt nanoparticles are formed. Unlike gold-ceria materials [8], the reduced platinum–ceria samples can not be reoxidized at ambient temperature by oxygen or water vapor.

Fig. 4 H₂-TPR cycles of (a) 2.2%PtCeLaQ (IMP); (b) 0.7%PtCeLaQ (IMP, NaCN); (c) 1.2%PtCeQ (IMP); (d) 0.8%PtCeQ (DP pH2); (e) 0.3%PtCeQ (DP pH12). Samples were purged in He at RT for 0.5 h before the first cycle. Test: 20% H₂/N₂; 50 cm³/min (NTP); 5 °C/min. The subsequent cycle was run after 20% O₂/He reoxidation at 350 °C for 0.5 h and purge with He



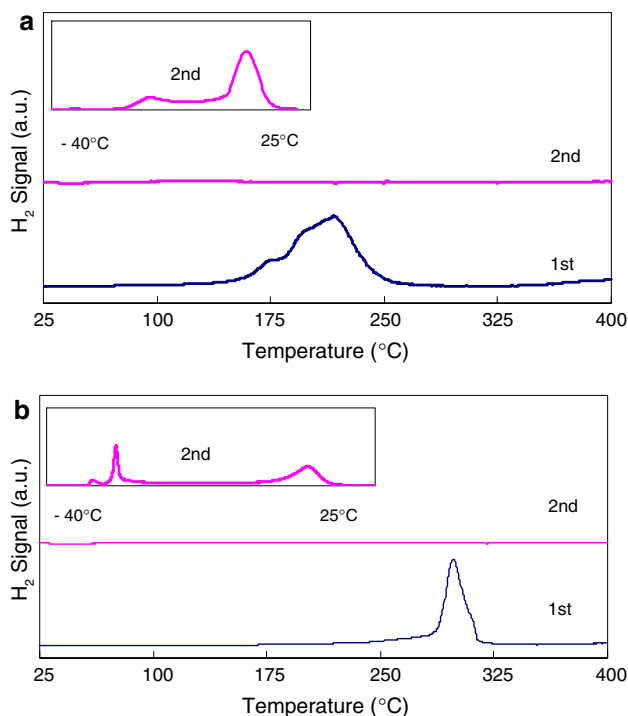


Fig. 5 H₂-TPR cycles of (a) 5.3%PtCeQ (UGC); (b) 1.1%PtCeQ (UGC). Samples were purged in He at RT for 0.5 h before the first cycle. Test: 20% H₂/N₂; 50 cm³/min (NTP); 5 °C/min. The subsequent cycle was run after 20% O₂/He reoxidation at 350 °C for 0.5 h and purge with He

0.8%PtCeQ shows hydrogen consumption of only 638 μmol/g_{cat} a 40% loss compared to the first cycle. In contrast, exposure of the catalyst to the full reformat gas (11%CO–26% H₂–26% H₂–7%CO₂–He) at 300 °C for 17 h retains more oxidized platinum in the sample than exposure to hydrogen (Line b in Fig. 6). This is corroborated by the TPR data for the used catalyst after 17 h time-on-stream (not shown). The hydrogen consumption over the reaction-used material is 954 μmol/g_{cat} a little less than the fresh, but much higher than in the second TPR cycle (638 μmol/g_{cat} Table 3).

The 5.3%PtCeQ(UGC) sample shows the highest H consumption value of 2040 μmol/g_{cat} while the 1.1%PtCeQ (UGC) sample follows with 1060 μmol/g_{cat}. Following reoxidation of these samples at 350 °C, a second cycle of TPR found their reduction profiles had shifted dramatically to temperatures lower than ambient. To capture this reduction, a dry ice-ethanol bath was used to lower the temperature to –40 °C and thereby suppress the immediate room temperature reduction. The cyclic reduction profiles of the 5.3%PtCeQ (UGC) sample are shown in Fig. 5a. There are two major reduction peaks seen as the sample heats in the H test gas up to room temperature from the sub-zero temperature giving a total reduction of 1,339 μmol/g_{cat}. No further reduction is observed from 25 °C to the final temperature of 400 °C.

An in situ H₂ reduction up to 400 °C was performed on both the UGC and the 2.2%PtCeLaQ(IMP) samples prior to exposure to WGS product-free reaction gases (see Fig. 6a). Following this in situ reduction process, all samples were more active for WGS than the fresh materials. This increased activity of the samples may be caused by either: (1) activation of the catalyst by the H₂ gas; or (2) exposure of the active sites by the removal of carbonates from the surface. To answer this, a fresh batch of 5.3%PtCeQ was oxidized in situ at 350 °C for 30 min prior to exposure to the WGS product-free gas. As can be seen in Fig. 6b, the preoxidized sample has a similar activated performance to that of the in situ reduced material. This demonstrates the surface carbonate decomposition as the reason for the catalyst activation shown in Fig. 6a and b.

The in situ reduced and WGS used 5.3%PtCeQ and 1.1%PtCeQ(UGC) samples were further subjected to a TPR experiment. A helium purge at RT for 0.5 h was the only pre-treatment of the used 5.3%Pt–CeQ sample before starting the TPR test. Unlike its behavior in cyclic TPR (Fig. 5a), the reaction used 5.3%Pt material had two distinct regions of reduction: a sub-RT and a high temperature one (Fig. 6c). Integration of the sub-RT reduction peak gave a consumption of H₂ of 581 μmol/g_{cat} and the high temperature one 1193 μmol H₂/g_{cat}. On the other hand, the used 1.1%PtCeQ

Table 3 Reducibility of Pt–CeQ materials^a

Catalyst	H ₂ -TPR			
	Cycle 1		Cycle 2	
	T _r ^b (°C)	H ₂ consumption (μmol/g)	T _r ^b (°C)	H ₂ consumption (μmol/g)
2.2%PtCeLaQ(IMP)	241	1099	162	1121
0.7%PtCeLaQ(IMP, NaCN)	294	809	65	505
1.2%PtCeQ(IMP)	261	988	81	744
0.8%PtCeQ(DP,pH2)	325	1037	78	638
0.3%PtCeQ(DP,pH12)	293	800	62	572
5.3%PtCeQ(UGC)	217	2040	<25	1339
1.1%PtCeQ(UGC)	298	1060	<25	947

^a Samples were purged in He at RT for 0.5 h before the first cycle. The subsequent cycle was run after 20% O₂/He reoxidation at 350 °C for 0.5 h

^b T_r is the peak temperature of the main reduction peak

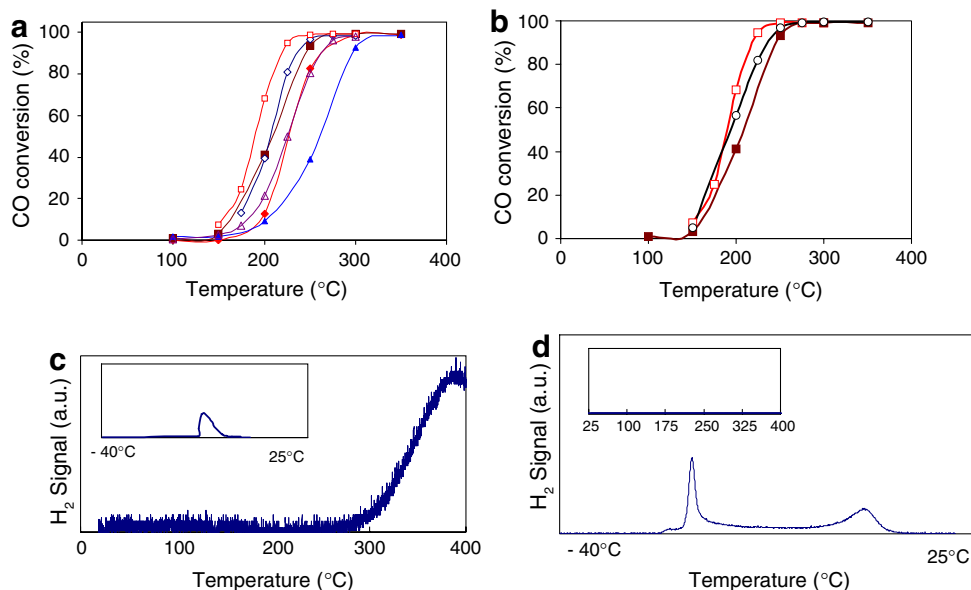


Fig. 6 (a) WGS light-off over the Pt-ceria catalysts; steady-state conversion measurements. Gas mixture: 2%CO–10.7%O₂–He; contact time: 0.09 g s/cc. Closed triangles—2.2%PtCeLaQ(IMP); Open triangles—in situ H₂ reduced 2.2%PtCeLaQ(IMP); Closed squares—5.3%PtCeQ(UGC); Open squares—in situ H₂ reduced 5.3%PtCeQ (UGC); Closed diamonds—1.1%PtCeQ(UGC), Open diamonds—in situ H₂ reduced 1.1%PtCeQ(UGC). In situ H₂ reduction: 20%H₂ at 5 °C/min from RT to 400°C; Cooled to 300°C in He for 30 min; WGSR tests from 300 to 150°C in descending temperature mode (b) WGS light-off over the 5.3%PtCeQ catalyst after various pretreatments; steady-state conversion measurements. Gas mixture: 2%CO–10.7%O₂–He; contact time: 0.09 g s/cc. Closed squares—Fresh 5.3%PtCeQ(UGC); Open squares—in situ H₂ reduced 5.3%PtCeQ(UGC); In situ H₂ reduction: 20%H₂ at 5 °C/min from RT to 400°C; Cooled to 300°C in He for 30 min; WGSR tests from 300 to 150°C in descending temperature mode. (c) H₂-TPR of used 5.3%PtCeQ(UGC). Used sample was recovered following in situ H₂ reduction/WGS reaction test at the conditions of a. The sample was purged in He at RT for 0.5 h before the TPR test. (d) H₂-TPR of used 1.1%PtCeQ(UGC). Used sample was recovered following in situ H₂ reduction/WGS experiment at the conditions of a. The sample was oxidized at 350°C in 20%O₂ for 0.5 h, followed by RT He sweep for 0.5 h before the TPR test

material was pre-treated at 350°C in oxygen followed by a helium sweep prior to starting the TPR test. In Fig. 6d, this sample only had the sub-RT reduction profile with a hydrogen consumption of 61 μmol/g_{cat}. We attribute this difference to carbonate formation. The He purge alone could not remove the carbonates from the 5.3%Pt sample. Upon exposure to high temperature (250 °C) during the TPR test, the carbonate was reduced allowing for further ceria surface reduction and hydrogen consumption. By contrast, the used 1.1%PtCeQ had its carbonates removed by the 350°C oxygen treatment, and its TPR profile (Fig. 6d) was similar to the second TPR cycle of this sample shown in Fig. 5c. While the carbonate presence lowers the catalyst activity, there is no long-term effect on the catalyst stability as the data of Fig. 3a demonstrate.

3.4 Stability in Shutdown-startup Operation

The stability of PtCeQ catalysts was further evaluated in shutdown/re-start cycles to simulate realistic fuel cell operation. In an earlier study, we found that the formation

of cerium(III) hydroxycarbonate causes the deactivation of gold-ceria catalysts during shutdown—startup [31]. However, we showed that addition of a small amount of oxygen in the WGSR gas mixture could inhibit the formation of cerium hydroxycarbonate, thus preventing the gold-ceria catalyst deactivation. By contrast, addition of 0.5% O₂ in a gas mixture of 10%CO–10%O₂–60%H₂–7%CO₂–He did not stabilize the WGS activity of a Pt–CeO catalyst [31]. It is possible that the oxygen potential in this particular gas mixture with very high H₂ content (60%) is not high enough to keep Pt–CeO surface free of carbonate. In Fig. 7a, the oxygen potential was changed by varying the ratio of O₂ to H₂. For the first 20 min, the reaction was carried out in the reformat gas mixture of 11% CO–26% H₂O–26% H₂–7% CO₂–He. After steady state was reached at 300°C, the sample was cooled to room temperature and held for 2 h before it was reheated to 300°C; all in the same flowing gas mixture. Addition of 1%O₂ in this gas mixture was enough to stabilize the 2.2%PtCeLaQ(IMP) catalyst and to prevent its better activity recovery than 0.5%O₂ which confirms that

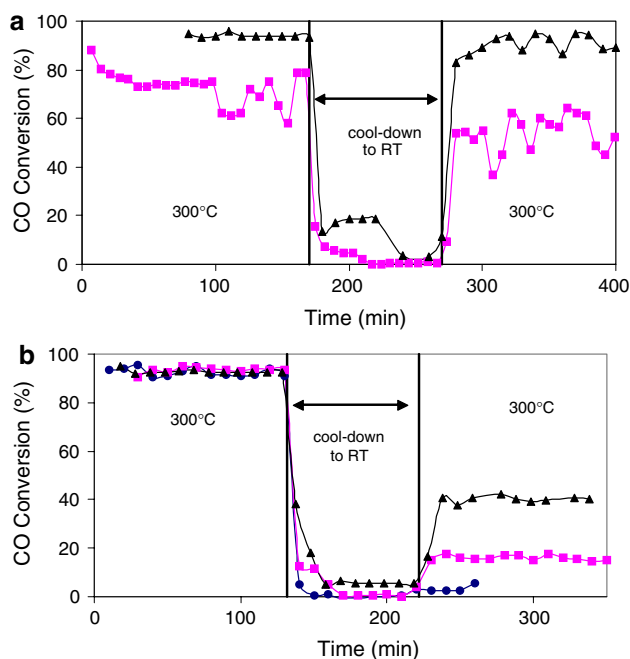


Fig. 7 WGSR shutdown/startup operation over a) 2.2%PtCeLaQ (IMP) and b) 5.3%PtCeQ (UGC) catalysts under various oxygen concentrations. Feed gas mixture: 11%CO–26% H_2 O–7%CO₂–He; S.V.= 50,000 h⁻¹; catalyst was tested at 300°C for 2 h, cooled to room temperature during shutdown with gas flowing for approximately 2 h, then reheated to 300°C. (a) squares: 0.5%O₂ in feed gas; triangles: 1.0%O₂ in feed gas. (b) circles: no O₂ in feed gas; squares: 0.5%O₂ in feed gas; triangles: 1.0%O₂ in feed gas

the oxygen potential is the key factor that controls the deactivation of ceria-based catalysts.

Interestingly, the UGC-prepared 5.3%PtCeQ requires an even higher oxygen partial pressure to be fully stabilized. As shown in Fig. 7b, when the oxygen content was varied from 0 to 0.5% and 1%, respectively, the activity recovery of this material varied from less than 5–20% and 40%. Compared to Au-ceria, Pt-ceria catalysts require a higher oxygen potential reaction gas to stabilize their WGS activity. This may be attributed to the over-reduction of ceria caused by platinum [26]. On the other hand, using lanthanum as a cerium oxide dopant, appears to be beneficial, judging from the higher shutdown/re-start stability of the 2.2%PtCeLaQ sample (comparing Fig. 7a and b). More detailed work on how different dopants may prevent the cerium carbonate formation is warranted.

4 Conclusions

Platinum–cerium oxide catalysts can be prepared by various methods, including IMP, DP and UGC, in a form that is both active and stable in low-temperature WGSR. The UGC method is particularly well suited to prepare nano-scale ceria with a higher amount of oxidized Pt species

strongly bound to ceria. The interaction produces near ceria nanoparticles and a higher amount of reactive surface oxygen. Activity is higher if either hydrogen or oxygen gas is used to pre-treat the catalysts, indicating the importance of carbonate removal from the catalyst surface. The oxidation state of the surface Pt species is determined by the oxidation potential of the reaction gas mixture. Some, but not all the platinum is in metallic state after use. This can be reoxidized by heating to temperatures up to 360

Oxygen gas addition (~1 mol%) in the reformat gas mixture can be used to inhibit the deactivation of the PtCeQ catalysts during RT shutdown/re-start cycles. Oxygen prevents the formation of cerium(III) hydroxycarbonate at low temperatures. The amount required may be related to the number of redox sites of ceria, but more work is required to probe this. Nonetheless, active and stable catalysts based on nanoscale ceria doped with a small amount of platinum can be developed for practical fuel cell applications.

Acknowledgments This work was supported by the National Science Foundation, NIRT Grant # 0304515; and by the Department of Energy, Basic Energy Sciences, Hydrogen Fuel Initiative Grant # DE-FG02-05ER15730. The authors would like to thank Elisabeth Shaw at MIT Center for Materials Science and Engineering for her help with the XPS analysis and Yanping Zhai for some of the WGS reaction rate measurements.

References

1. Shelef M, George W, Graham W, McCabe RW (2002) In: Trovarelli A (ed) Catalysis by ceria and related materials, Catalytic Science Series, vol 2. Imperial College Press, p 343
2. Zhu T, Kundakovic Lj, Dreher A, Flytzani-Stephanopoulos M (1999) Catal Today 50:381
3. Liu W, Flytzani-Stephanopoulos M (1995) J Catal 153:304
4. Liu W, Flytzani-Stephanopoulos M (1995) J Catal 153:317
5. Murrell LL, Tauster SJ, Anderson DR (1991) In: Cruick A (ed) Catalysis and automotive pollution control II. Elsevier Science Publishers, p 275
6. Hardacre C, Ormerod RM, Lambert RM (1994) J Phys Chem 98:10901
7. Fu Q, Saltsburg H, Flytzani-Stephanopoulos M (2003) Science 301:935
8. Fu Q, Deng W, Saltsburg H, Flytzani-Stephanopoulos M (2005) Appl Catal B 56:57
9. Yao H-C, Yu Yao FY (1984) J Catal 86:254
10. Bunluesin T, Cordatos H, Gorte RJ (1995) J Catal 157:222
11. Bunluesin T, Gorte RJ, Graham GW (1998) Appl Catal B 15:107
12. Kundakovic Lj, Flytzani-Stephanopoulos M (1998) J Catal 179:203; Martínez-Arias A, Fernández-García M, Gávez O, Coronado JM, Anderson JCA, J Catal 195:207
13. Li Y, Fu Q, Flytzani-Stephanopoulos M (2000) Appl Catal B 27:179
14. Avgouropoulos G, Ioannides T, Papadopoulou C, Batista J, Hocevar S, Matralis HK (2002) Catal Today 75:157
15. Fu Q, Weber A, Flytzani-Stephanopoulos M (2001) Catal Lett 77(1–3):87

16. Tabakova T, Boccuzzi F, Manzoli M, Andreeva D (2003) Appl Catal A 252(2):385
17. Tabakova T, Boccuzzi F, Manzoli M, Sobczak JW, Idakiev V, Andreeva D (2004) Appl Catal B 49:73
18. Fu Q, Kudriavtseva S, Saltsburg H, Flytzani-Stephanopoulos M (2003) Chem Eng J 93:41
19. Fu Q (2004) Ph.D. dissertation, Department of Chemical and Biological Engineering, Tufts University, Medford, MA
20. Yeung CMY, Yu KMK, QJ Fu D, Thompsett, Petch MI, Tsang SC (2005) JACS 127(51):18010
21. Chiang YM, Lavik EB, Kosacki I, Tuller HL, Ying JY (1997) J Electroceramics 1:7
22. Kek-Merl D, Lappalainen J, Tuller HL (2006) J Electrochem Soc 153(3):J15
23. Carretin S, Concepcion P, Corma A, Lopez Nieto JM, Puentes VF (2004) Angew Chem Int Ed 43:2538
24. Guzman J, Carretin S, Corma A (2005) JACS 127:3287
25. Kim CH, Thompson LT (2005) J Catal 230:66
26. Zalc JM, Sokolovskii V, Lof er DG (2002) J Catal 206:169
27. Wang X, Gorte RJ, Wagner JP (2002) J Catal 212:225
28. Hillaire S, Wang X, Luo T, Gorte RJ, Wagner JP (2001) Appl Catal A 215:271
29. Liu X, Ruettinger W, Xu X, Farrauto R (2005) Appl Catal B 56:69
30. Ruettinger W, Liu X, Farrauto R (2002) US patent 141938
31. Deng W, Flytzani-Stephanopoulos M (2006) Angew Chem Int Ed 45:2285
32. Deng W, De Jesus J, Saltsburg H, Flytzani-Stephanopoulos M (2005) Appl Catal A 291:126
33. Deng W (in progress) Ph.D. thesis
34. <http://www.webelements.com>
35. Zhang F, Chan S-W, Spanier JE, Apak E, Jin Q, Robinson RD, Herman IP (2002) Appl Phys Lett 80(1):127
36. Manzoli M, Boccuzzi F, Chiorino A, Vindigni F, Deng W, Flytzani-Stephanopoulos M (2007) J Catal 245(2):308